

## Large coercivity and surface anisotropy in MgO/Co multilayer films

Jian-Wang Cai, Satoshi Okamoto, Osamu Kitakami, and Yutaka Shimada

*Research Institute for Scientific Measurements, Tohoku University, Katahira 2-1-1, Aoba-ku, Sendai 980-0812, Japan*

(Received 20 June 2000; published 20 February 2001)

The multilayer films of  $(30 \text{ \AA} \text{ MgO}/12\text{--}65 \text{ \AA} \text{ Co})_{30}$  were deposited on oxide-coated Si(100) wafers in a UHV chamber by rf and dc sputtering. Structural analyses reveal that the films with Co layer thickness ( $t_{\text{Co}}$ ) above 16 \AA have well-defined layer structure, however, Co layers become discontinuous to some extent when  $t_{\text{Co}}$  is down to 12 \AA. MgO layers are (100) oriented, and Co layers have fcc phase with fcc(200) parallel to MgO(200) when  $t_{\text{Co}}$  is below 20 \AA, but the hcp phase is stabilized in thicker Co layers ( $25 \text{ \AA} \leq t_{\text{Co}} \leq 65 \text{ \AA}$ ) with hcp(110) parallel to MgO(200). There is no evidence of exchange bias stemming from the oxidation of Co, and all films exhibit planar magnetization. Coercivity of higher than 12 kOe was observed at 10 K for  $t_{\text{Co}} = 12 \text{ \AA}$ , which is far beyond the effective magnetocrystalline anisotropy field of fcc or hcp Co. The thickness dependence of coercivity at 10 K follows a linear scale as  $1/t_{\text{Co}}$ . With the increase of the temperature, the coercivity decreases, and the maximum value at room temperature is about 420 Oe for  $t_{\text{Co}} = 25 \text{ \AA}$ . A proposal to evaluate the surface anisotropy via initial susceptibility measurement along the film normal direction for a film with planar magnetization is presented. Surface anisotropy is thus determined to be about 1.3 erg/cm<sup>2</sup> at 10 K and 0.4 erg/cm<sup>2</sup> at room temperature with the film normal as the hard axis. Surface anisotropy has been demonstrated to be a dominant term to determine the magnetic behavior of MgO/Co multilayer films, especially at low temperature.

DOI: 10.1103/PhysRevB.63.104418

PACS number(s): 75.50.Vv, 75.30.Gw, 75.70.Ak

### I. INTRODUCTION

High density magnetic recording media primarily requires a high coercivity to overcome demagnetizing fields that tend to destabilize the magnetization of the recorded bits and weakly exchange coupled fine grains to obtain a satisfactory signal-to-noise ratio. Future generation 100 Gbits/in<sup>2</sup> magnetic media would need to have a coercivity higher than 4 kOe, and well-isolated grains of less than 10 nm in size, which approaches an intrinsic physical limit on grain size, i.e., the superparamagnetic limit. In order to retain thermal stability, magnetic anisotropy  $K_u$  as high as  $10^7$  erg/cm<sup>3</sup> is a prerequisite in such small particles.<sup>1,2</sup> As a consequence, magnetic granular systems containing ordered equiatomic CoPt and FePt, which have extremely high anisotropy,<sup>3,4</sup> have attracted particular interest recently.<sup>5-8</sup> On the other hand, surface effects occur with the reduction of the sample dimension. This might be an important source to enhance the magnetic anisotropy and alter the magnetic behavior in the nanostructures. Up to date, extensive investigations have been concentrated on the perpendicular anisotropy in multilayer films being composed of transition metal ferromagnets (FM) Fe, Co, Ni, etc, and nonmagnetic (NM) metals Cu, Ag, Au, Pt, Pd, etc.<sup>9</sup> Indeed, surface anisotropy in some cases is strong enough to overwhelm the tendency of in-plane magnetization favored by the strong magnetostatic shape anisotropy and switch the easy axis of magnetization perpendicular to the film plane. Meanwhile, some evidence indicates that the nanostructured FM/oxide interface plays a critical role in determining a system's properties. For example, the coercivity of an ultrathin Co film with perpendicular magnetization was found to decrease to less than  $\frac{1}{6}$  of its magnitude upon coverage of a 30 \AA MgO layer,<sup>10</sup> whereas large coercivity in Fe/SiO<sub>2</sub> granular films could be interpreted only by taking into account surface anisotropy.<sup>11</sup>

Nevertheless, Co spin polarization in the magnetic tunneling junctions can even vary from positive to negative because of the different bonding effects at the interface of Co and oxides.<sup>12,13</sup> It can be expected that the nanostructured FM/oxide interface produces rather complex properties, which will open a possible way to explore novel physics and exploit exciting applications.

Because of the relatively high magnetic anisotropy, a variation of magnetic properties, and some different phases depending on preparation conditions, ferromagnetic metal Co as well as Co-based alloys is especially highlighted. Since magnesium oxide has a very simple crystal structure and is chemically very stable, we thus multilayered a Co film by inserting MgO layers. In this article, we present features of the structural and magnetic properties of MgO/Co multilayer films.

### II. EXPERIMENT

The multilayer films of MgO/Co were prepared in a multisource magnetron sputtering system with a base pressure of  $<3 \times 10^{-9}$  Torr. Sputtering was administered in a very pure Ar (>99.9995%) atmosphere of 2.8 mTorr at ambient temperature with rf and dc power inputs of 55 and 6 W for high pure MgO (99.9%) and Co(99.9%) targets, respectively. The resulting deposition rates were 0.4 \AA/sec for MgO and 0.5 \AA/sec for Co. In this study, all samples consist of 30 bilayers of MgO/Co and a cap layer of 120 \AA MgO, which were grown on native oxide-coated Si(100) wafers for structural characterization and magnetic measurements, or on polyimide films for cross-section transmission electron microscopy (XTEM) observations. The Co thickness was varied from 12 to 65 \AA, and the MgO thickness was kept constant and equal to 30 \AA from one multilayer to another. The microstructure was examined with a Hitachi H-700H transmission electron

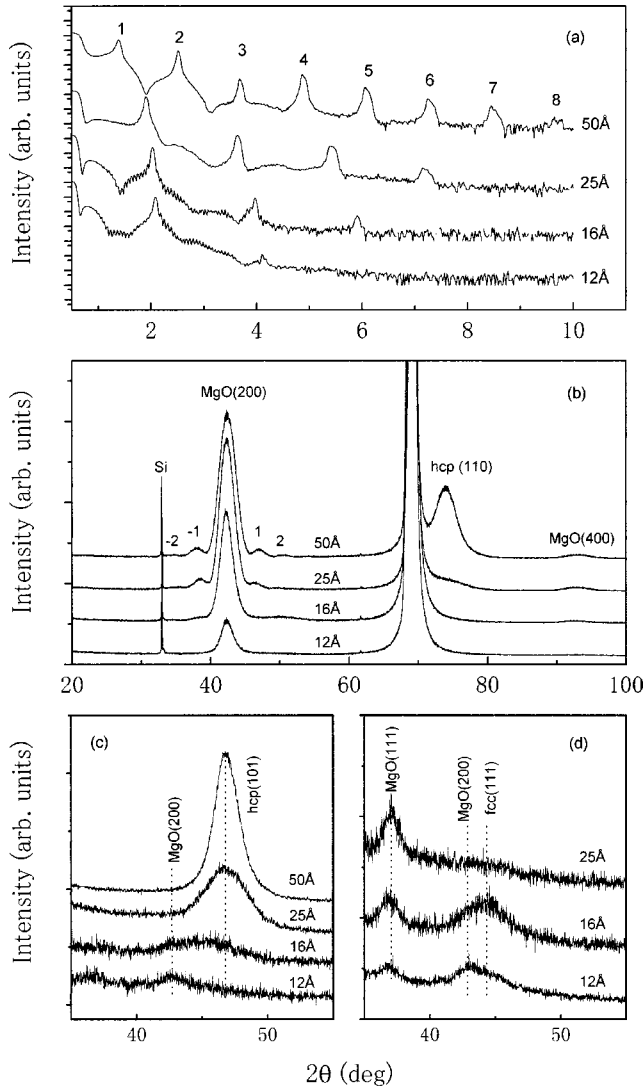


FIG. 1. X-ray scattering spectra for (a) low-angle x-ray diffraction, (b) high-angle x-ray standard  $2\theta/\theta$  scans, (c)  $2\theta/\theta$  scans with sample tilted at  $\psi=40.2^\circ$ , (d)  $2\theta/\theta$  scans with sample tilted at  $\psi=54.7^\circ$ .

microscopy operated at 200 kV with magnifications of 200 000 times. X-ray diffraction spectra were collected with a Philips X'Pert Materials Research Diffractometer (X'Pert-MRD) and a Rigaku powder diffractometer, both using  $\text{CuK}\alpha$  radiation. The electric resistivity was determined by the four-probe technique. Magnetic hysteresis loops and ac and dc susceptibilities were obtained via a vibrating sample magnetometer (VSM), a Quantum Design Physical Properties Measurement System (PPMS), and a Quantum Design superconducting quantum interference device (SQUID) magnetometer.

### III. STRUCTURAL CHARACTERIZATION

The structures of all samples were examined by x-ray diffraction. In Fig. 1(a), low-angle x-ray diffraction patterns of representative MgO/Co multilayers are shown. A large number of artificial structure peaks are observable for the

films with relatively thick Co layers, however, the high order peaks gradually disappear with the decrease of Co thickness, and the diffraction peaks only up to the second order are visible for the multilayers with  $t_{\text{Co}}=12\text{ \AA}$ . On the other hand, the bilayer thickness, determined from the peak position, agrees very well with the designed value. These results indicate that the layered structure profile is somewhat poor when the Co layer is very thin, but it improves greatly with increasing Co thickness. Figure 1(b) shows the standard high-angle x-ray  $2\theta/\theta$  scattering spectra for the representative multilayers. Several features are noted. MgO layers are (200) textured in all these multilayers, and the texture becomes stronger with increasing Co thickness until  $t_{\text{Co}}=20\text{ \AA}$ , at which it almost saturates. There are several satellite peaks near MgO(200) for  $t_{\text{Co}}>16\text{ \AA}$  because of the high quality of the artificial structure. From the width of the MgO(200), beyond the instrumental width, the structural coherence length has been determined to be about  $35\text{ \AA}$  for all samples, a little larger than MgO thickness, which means that the coherent growth throughout the whole film does not take place. Except the strong MgO(200) and some satellite peaks, a very weak and broad peak around  $51.1^\circ$  was found for multilayers with  $t_{\text{Co}}$  less than  $20\text{ \AA}$ , but it disappears or might be submerged in the satellite peaks as Co thickness increases, meanwhile, another peak around  $75.1^\circ$  appears and grows to be very sharp. The former seems to come from Co fcc(200), whereas the latter cannot be identified as Co fcc(220) or hcp(110) because the two peaks are very close to each other. One can easily calculate that the hcp(101) plane is at an angle of  $40.2^\circ$  with respect to hcp(110) for Co. So if there are oriented hcp Co grains with the (110) planes parallel to the film plane, the x-ray scattering peak from the hcp(101) plane should be observed by tilting the film normal by  $40.2^\circ$  with respect to the x-ray incident plane. The tilt angle is denoted as  $\psi$ . Since the angle between fcc(220) and (111) planes is  $35.3^\circ$ , and that between fcc(200) and (111) planes is  $54.7^\circ$ , we performed a series of  $2\theta/\theta$  scans with  $\psi=35.3^\circ$ ,  $40.2^\circ$ , and  $54.7^\circ$  for all samples, where an attachment for pole figure data collection was used for the primary optics, and a parallel plate collimator used for diffracted beam. There is no observable peak near  $44.2^\circ$  for all samples when  $\psi=35.3^\circ$ , so any possibility of a (220) oriented fcc Co layer is eliminated. When samples were tilted at  $\psi=40.2^\circ$ , an appreciable peak at  $47.5^\circ$  corresponding to Co hcp(101) was found only for  $t_{\text{Co}}\geq 25\text{ \AA}$ . As can be seen clearly in Fig. 1(c), the hcp(101) peak becomes very sharp with increasing Co thickness. On the other hand, one can note that in Fig. 1(d), the tilting sample at  $\psi=54.7^\circ$  does not result in the occurrence of a fcc(111) peak for  $t_{\text{Co}}>20\text{ \AA}$ , but a fcc(111) peak does appear for  $t_{\text{Co}}<20\text{ \AA}$  although it is very weak. So the fcc phase is stabilized in thin Co layers ( $12\text{ \AA}\leq t_{\text{Co}}<20\text{ \AA}$ ) with the fcc(200) plane parallel to the MgO(200) plane. The weak fcc peaks for both normal and tilt scans suggest that Co grains in this thickness region are very fine, which may come partly from the large mismatch between MgO(200) and Co fcc(200). With the increase of the Co thickness, (110) oriented hcp Co is convincingly confirmed. We would like to point out that the unit cell of Co hcp(110),  $4.342\text{ \AA}\times 4.070\text{ \AA}$ , matches MgO(200) quite well,

$4.213 \text{ \AA} \times 4.213 \text{ \AA}$ , which gives rise to the strongly (110) preferred orientation for thick Co layers.

Although low-angle x-ray diffraction provides the most important evidence about the layer structure, electric resistivity can offer some supplementary information. It should be noted that all Co layers contribute to the conductivity because of the connection between neighboring Co layers at the film edges or at other perturbations. The resistivity for  $(30 \text{ \AA} \text{ MgO}/65 \text{ \AA} \text{ Co})_{30}$  is thus determined to be about  $50 \mu\Omega \text{ cm}$ , which is somewhat higher than the value for bulk Co because of the defects and/or stress in the multilayered films. With the decrease of Co thickness, the resistivity gradually increases until  $t_{\text{Co}}=25 \text{ \AA}$ , at which the resistivity is about  $100 \mu\Omega \text{ cm}$ . Further decreasing Co thickness results in a much faster increase of the resistivity, and a percolation limit for Co layer was found near  $12 \text{ \AA}$ .

Based upon above x-ray scattering results and resistivity measurements, a picture for the layer structures of MgO/Co multilayers could be proposed. Since the surface free energy of Co is much higher than that of MgO, each Co layer tends to form fcc islands with (200) parallel to MgO(200) at the early stage of the growth.<sup>14</sup> These individual islands will grow gradually, but most of them do not impinge on each other until the Co layer reaches a critical thickness. This is the case for  $t_{\text{Co}} \leq 12 \text{ \AA}$ . As the Co thickness increases, the Co layer becomes continuous, and the larger the thickness, the flatter the layer of Co until  $t_{\text{Co}}=20 \text{ \AA}$ . On the other hand, MgO seems to wet Co because of the very high melting point of MgO.<sup>15,16</sup> Therefore, thicker Co layers with improved morphology lead to sharper layer profiles, which was observed in the x-ray diffraction. Since the mismatch between fcc Co(200) and MgO(200) is very large, and fcc Co itself is metastable at room temperature, Co layers, for a lower energy state when  $t_{\text{Co}} \geq 25 \text{ \AA}$ , transform to hcp phases with the (110) plane parallel to the MgO(200) plane, which perfectly matches as described before.

The above picture of the evolution of the microstructure with the variation of Co thickness is further confirmed by XTEM on almost half of the multilayers. Figure 2 shows the representative electron micrographs. First we would like to mention that the large long scale roughness on both sides of the film is just an effect of the sample preparation process for XTEM, and no columnar growth takes place for the MgO/Co multilayers, which is consistent with the high-angle x-ray diffraction results. The XTEM micrographs clearly show that the multilayers with  $t_{\text{Co}} > 20 \text{ \AA}$  have high structural perfection with a surprisingly flat interface, however, a much less perfect layer structure happens for the sample with  $t_{\text{Co}} = 12 \text{ \AA}$ , where the Co layer is discontinuous to some extent although the feature of layer structure remains observable.

#### IV. MAGNETIC PROPERTIES

Magnetic hysteresis loops at room temperature (RT) and 10 K were measured. All samples exhibit planar magnetization without perpendicular anisotropy.  $M$ - $H$  curves with the external field along the film normal are straight lines before turning to saturation, where no remanent magnetization is evident. The hysteresis in this article was obtained with an

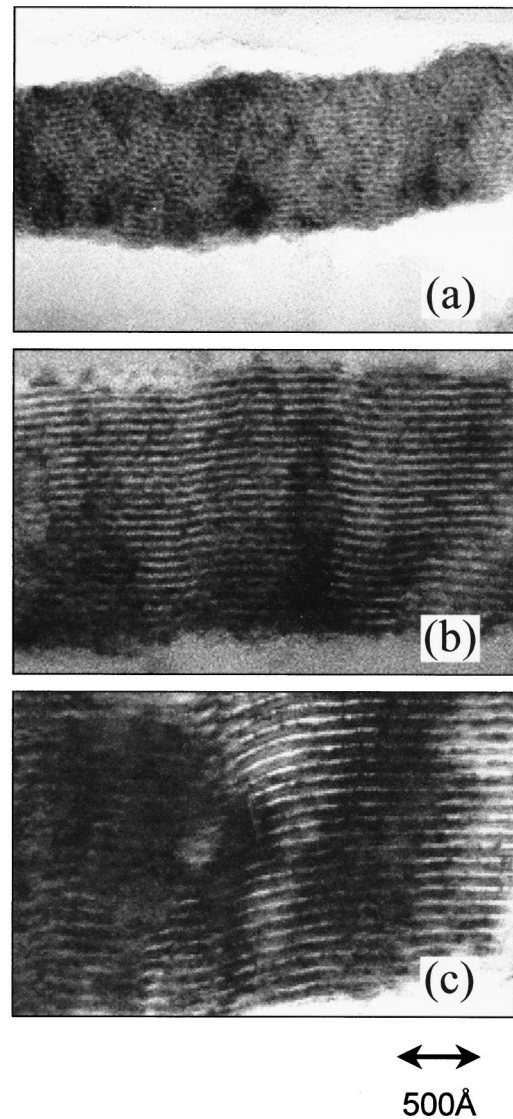


FIG. 2. Cross-section transmission electron micrographs for multilayers of (a)  $t_{\text{Co}} = 12 \text{ \AA}$ , (b)  $t_{\text{Co}} = 25 \text{ \AA}$ , and (c)  $t_{\text{Co}} = 50 \text{ \AA}$ .

external field in the film plane. Figure 3(a) shows the Co thickness dependence of coercivity at room temperature. The coercivity is null for  $t_{\text{Co}} = 12 \text{ \AA}$ . With the increase of Co thickness, the coercivity rapidly rises to 420 Oe for  $t_{\text{Co}} = 25 \text{ \AA}$ , then it decreases gradually. From the  $M$ - $H$  curves depicted in the inset of Fig. 3(a), the feature of no hysteresis in the multilayers of  $(30 \text{ \AA} \text{ MgO}/12 \text{ \AA} \text{ Co})_{30}$  reminds one of superparamagnetism, which is convincingly demonstrated by a comprehensive examination of its magnetic behavior presented in detail later. The superparamagnetism is suppressed with the increase of Co thickness, and the coercivity and remanent magnetization ratio thus increase until  $t_{\text{Co}} = 25 \text{ \AA}$ . For the multilayers with  $t_{\text{Co}} \geq 25 \text{ \AA}$ , the hysteresis loops have a similar shape with a remanent magnetization ratio of about 0.8. A representative loop for  $t_{\text{Co}} = 25 \text{ \AA}$  is also shown in the inset of Fig. 3(a). Coercivity in this thickness region, mainly determined by the domain nucleation or pinning of domain walls through local anisotropy, monotonically decreases with increasing Co thickness.

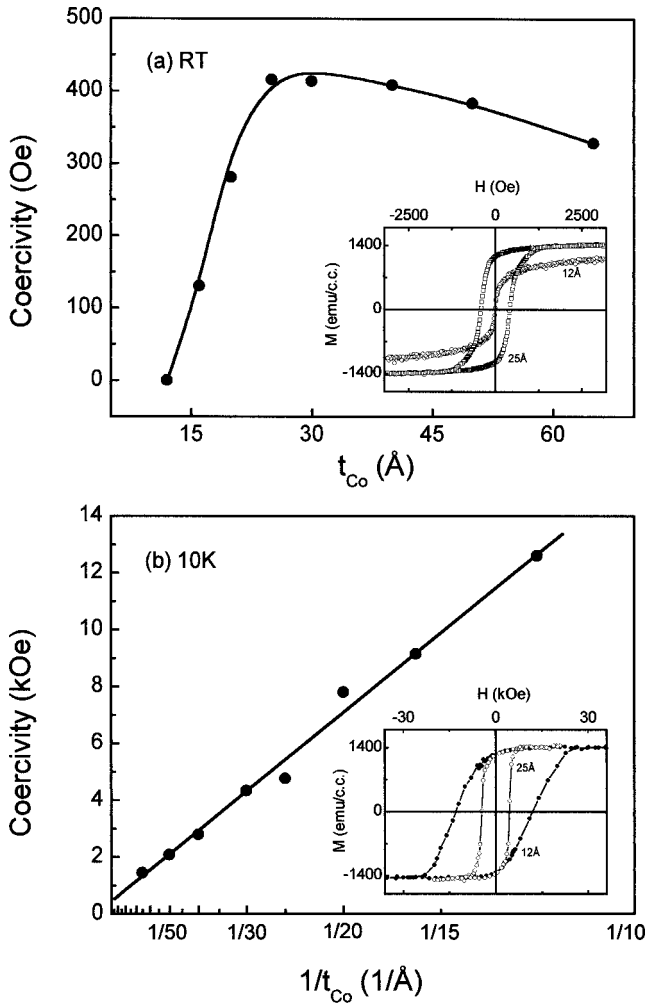


FIG. 3. (a) Thickness dependence of coercivity at room temperature, (b) Variation of coercivity at 10 K as a function of reciprocal thickness of Co layer. The hysteresis loops for  $t_{\text{Co}}=12$  and  $25 \text{ \AA}$  at room temperature and 10 K are displayed in the insets of (a) and (b), respectively.

In Fig. 3(b), the coercivity at 10 K is plotted as a function of the reciprocal Co thickness. Two hysteresis loops corresponding to  $t_{\text{Co}}=12$  and  $25 \text{ \AA}$  at 10 K are also displayed in the inset of Fig. 3(b). Several features are noted. A huge coercivity of  $12.6 \text{ kOe}$  was found for  $(30 \text{ \AA MgO}/12 \text{ \AA Co})_{30}$ . To the best of our knowledge, this is the largest coercivity for Co multilayer films with or without perpendicular anisotropy. The value of coercivity falls with increasing Co thickness, and follows a linear scale as  $1/t_{\text{Co}}$  perfectly in the whole thickness region from 12 to  $65 \text{ \AA}$ . The hysteresis loops for quite a few samples were measured after cooling the samples from room temperature with an external field of  $30 \text{ kOe}$ , however, no exchange bias was found for all of them. So the great enhancement of the coercivity for MgO/Co multilayers at low temperature could not stem from the coupling with antiferromagnetic CoO surface layers. Since the large coercivity is even much higher than the effective magnetocrystalline anisotropy field for fcc or hcp Co, some other sources that contribute to the anisotropy energy must exist. From the x-ray diffraction, both fcc and hcp

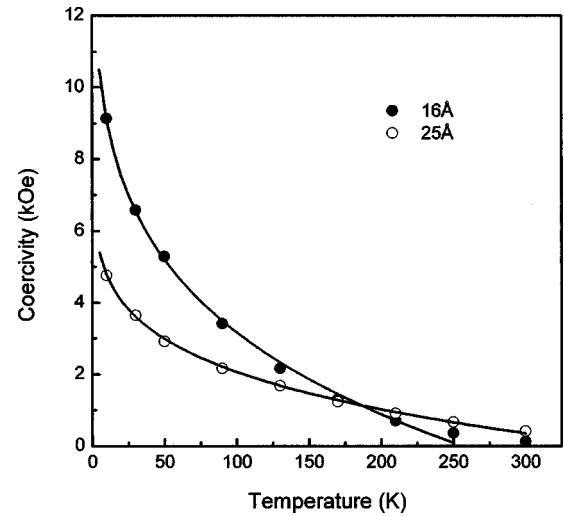


FIG. 4. Temperature dependence of coercivity for  $t_{\text{Co}}=16$  and  $25 \text{ \AA}$ . The solid lines are the fitting results with  $\nu = \frac{1}{6}$ .

peaks for Co layers in different thickness regions were found to shift to lower angles slightly, which means that Co layers are somehow compressively stressed, only a small negative magnetoelastic anisotropy is expected if the magnetostriction constant of bulk Co is assumed. Since the interface layers could be partially alloyed, the magnetostriction constant of Co may not necessarily be bulklike. A large strain at the first interface layer, which relaxes at the next layers, will give rise to a surfacelike anisotropy. In order to make this clear, samples with constant MgO and Co layer thickness but varying number of bilayers (from 10 to 30) were prepared. The magnetic measurements show that the coercivity is independent of the number of MgO/Co bilayers, which means that there is little possibility for the surfacelike anisotropy induced by the large strain at the first interface layer. The large coercivity and its behavior suggest that a large surface effect occur at MgO/Co interfaces.

Coercivity decreases for all multilayers as temperature is raised, and the thinner the layer of Co, the faster the decrease. The value of coercivity at relatively low temperature can be fitted by

$$H_C = \frac{a}{t_{\text{Co}}} \left[ 1 - \left( \frac{bT}{t_{\text{Co}}} \right)^\nu \right] \quad (0.1 < \nu < 0.2),$$

where  $T$  is temperature and  $a$ ,  $b$  are constants for different samples. Figure 4 displays the temperature dependence of coercivity for  $t_{\text{Co}}=16$  and  $25 \text{ \AA}$ , where solid lines are the fitting results with  $\nu = \frac{1}{6}$ . As is well known, the energy barriers, which uniquely determine magnetic reversal process at low temperature, can be overcome by the thermal fluctuation at elevated temperature. Thermal activation and probably reduced surface anisotropy seem to be responsible for the drastic decrease of coercivity as temperature rises. Gaunt<sup>17</sup> investigated domain wall pinning by a random array of inhomogeneities, and predicted that the effect of thermal activation on coercivity by  $H_C^{1/2} = H_0^{1/2}(1 - \text{const} \times T^{2/3})$  for the strong pinning model, and  $H_C = H_0(1 - \text{const} \times T)$  for the weak pinning model with the assumption of magnetization,

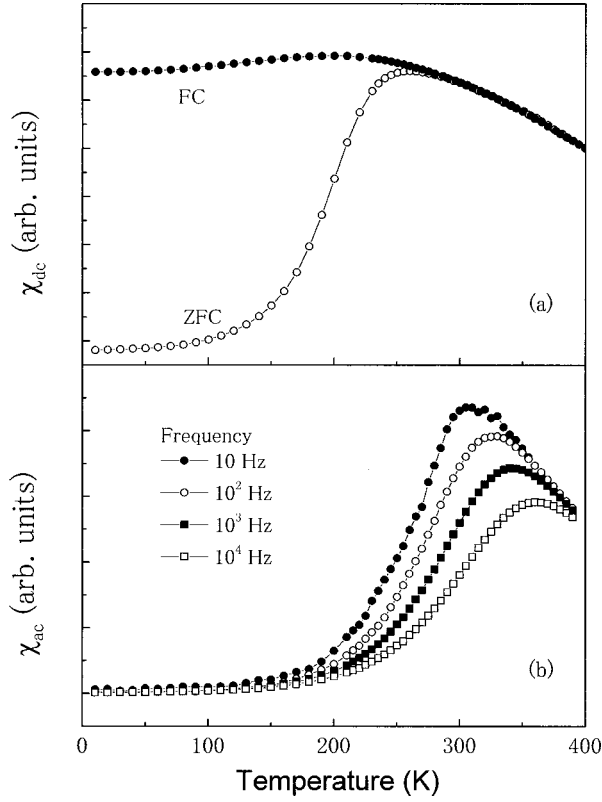


FIG. 5. (a) Field-cooled and zero-field-cooled dc susceptibility versus temperature with an applied field of 100 Oe, (b) Temperature dependence of ac susceptibility with the frequency varying from 10 to  $10^4$  Hz.

exchange, and anisotropy energies unvarying with temperature. Neither model is applicable to the multilayers of MgO/Co. In magnetic ultrathin films, a finite size effect may occur, and surface or interface roughness and defects become very important for the magnetic reversal process, so any model to describe the hysteresis properties of ultrathin films must take these features into account.

Although magnetic hardness is established for multilayers of  $(30 \text{ \AA} \text{ MgO}/12 \text{ \AA} \text{ Co})_{30}$  at low temperature, thermal activation seems to become the key issue at room temperature. In order to demonstrate this point convincingly, dc and ac susceptibility ( $\chi$ ) measurements were performed. Figure 5(a) is the variation of dc susceptibility with temperature for two different initial conditions. The curve denoted FC is for the sample initially cooled from 400 to 5 K in the presence of a 100 Oe external field, and for which the susceptibility was measured in the same field during the warming process. The ZFC curve is for the sample initially cooled in zero field and then measured in a field of 100 Oe. A cusp in dc susceptibility is evident for the ZFC curve, below which an irreversible difference between FC and ZFC magnetization occurs. We further studied its relaxation process by ac susceptibility. Figure 5(b) shows the temperature dependence of ac susceptibility at different ac frequencies. One observes that the ac susceptibility peak shifts to higher temperature as the frequency goes up. Superparamagnetism and the associated blocking phenomenon have thus been confirmed for  $(30 \text{ \AA} \text{ MgO}/12 \text{ \AA} \text{ Co})_{30}$ .

The surface effect is indispensable to account for the hysteresis behavior of MgO/Co multilayers at low temperature. We present the evaluation of the surface anisotropy below. The magnetocrystalline anisotropy for hexagonal crystals is generally expressed as

$$E_a = K_1 \sin^2 \alpha + K_2 \sin^4 \alpha,$$

where  $\alpha$  is the angle between magnetization vector and the  $c$  axis. When the (110) plane is taken as the  $x$ - $y$  plane for another coordinate system, the above expression is rewritten as

$$E_a = \left( \frac{1}{2} K_1 + \frac{3}{8} K_2 \right) + \left( \frac{1}{2} K_1 + \frac{1}{4} K_2 \right) \sin^2 \theta + \frac{3}{8} K_2 \sin^4 \theta \\ - \left( \frac{1}{2} K_1 + \frac{1}{2} K_2 + \frac{1}{2} K_2 \sin^2 \theta \right) \cos^2 \theta \cos 2\varphi \\ + \frac{1}{8} K_2 \cos^4 \theta \cos 4\varphi,$$

where  $\theta$  is the angle between the magnetization vector and the (110) plane, and  $\varphi$  is the azimuthal angle of the magnetization in the (110) plane with respect to the  $c$  axis. For (110) oriented polycrystalline films,  $\cos 2\varphi$  and  $\cos 4\varphi$  are averaged to be zero. If the film normal is the hard axis of the magnetization (including the shape anisotropy), an external field  $H$  applied perpendicular to the film plane will drag the magnetization out of the film plane, which is determined by

$$T = - \frac{\partial(E_a + E_d + E_H)}{\partial \theta} = 0,$$

where  $E_d = \frac{1}{2}(4\pi M_s^2) \sin^2 \theta$  (demagnetization energy),  $E_H = -M_s H \sin \theta$  (Zeeman energy).

The equilibrium condition for the magnetization is thus given by

$$\left( k_1 + \frac{1}{2} k_2 + 4\pi \right) m + \frac{3}{2} k_2 m^3 - h = 0,$$

where

$$m = \sin \theta, \quad k_1 = \frac{K_1}{M_s^2}, \quad k_2 = \frac{K_2}{M_s^2}, \quad \text{and} \quad h = \frac{H}{M_s}.$$

By differentiating the above equation, one obtains the susceptibility of hexagonal (110) oriented films as

$$\chi = \frac{1}{\left( k_1 + \frac{1}{2} k_2 + 4\pi \right) + \frac{9}{2} k_2 m^2}.$$

For cubic crystals, similarly, the magnetocrystalline anisotropy can be expressed in terms of  $\theta$ , the angle between magnetization vector and (100) plane, and  $\varphi$ , the azimuthal angle of the magnetization in (100) plane with respect to [100] crystallographic axis, i.e.,

$$E_a = \frac{1}{8}K_1 + \left(\frac{3}{4}K_1 + \frac{1}{8}K_2\right)\sin^2\theta - \left(\frac{7}{8}K_1 + \frac{1}{4}K_2\right)\sin^4\theta + \frac{1}{8}K_2\sin^6\theta - \left(\frac{1}{8}K_1 + \frac{1}{8}K_2\sin^2\theta\right)\cos^4\theta\cos 4\varphi.$$

The equilibrium condition for the magnetization of cubic (100) oriented films with an external field perpendicular to the film surface is derived to be

$$\left(\frac{3}{2}k_1 + \frac{1}{4}k_2 + 4\pi\right)m - \left(\frac{7}{2}k_1 + k_2\right)m^3 + \frac{3}{4}k_2m^5 - h = 0$$

and the susceptibility is given by

$$\chi = \frac{1}{\left(\frac{3}{2}k_1 + \frac{1}{4}k_2 + 4\pi\right) - 3\left(\frac{7}{2}k_1 + k_2\right)m^2 + \frac{15}{4}k_2m^4}.$$

Therefore, by measuring the susceptibility and magnetization in the film normal direction, one can determine anisotropy constants for hexagonal (110) or cubic (100) oriented films with planar magnetization. A very simple expression of the initial susceptibility is given by

$$\chi_0 = \frac{1}{k_v + 4\pi},$$

where  $k_v = k_1 + \frac{1}{2}k_2$  for hexagonal (110) films and  $\frac{3}{2}k_1 + \frac{1}{4}k_2$  for cubic (100) films. In thin films, surface or interface anisotropy becomes important. A phenomenological description of the surface or interface contribution to the magnetic anisotropy is given by

$$E_s = \frac{2}{t}K\sin^2\theta,$$

where  $\theta$  is the angle between the magnetization and film plane, and  $t$ , the thickness of magnetic layers. We use the same sign notation as introduced by Néel in his pioneering work,<sup>18</sup> where positive  $K_s$  means that the film normal is the hard axis. By performing the same procedure as described above, one obtains the initial susceptibility while considering surface anisotropy:

$$\chi_0 = \frac{1}{(4/t)k_s + k_v + 4\pi},$$

where  $k_s = K_s/M_s^2$ . The value of  $k_s$  can be easily extracted by plotting  $1/\chi_0 \sim 1/t$ . We would like to stress that the *perpendicular susceptibility* method can be applied only to the thin films with planar magnetization. This is the case for MgO/Co multilayers.

The initial perpendicular susceptibility was measured for all samples from 10 K to room temperature with an ac field amplitude of 10 Oe and a frequency of 1000 Hz. Figure 6(a) displays the reciprocal  $\chi_0$  as a function of the reciprocal Co thickness at 10 K and room temperature. A linear dependence of  $1/\chi_0$  on  $1/t_{Co}$  was found for  $t_{Co} \geq 25 \text{ \AA}$ , however, the data points for  $t_{Co} \leq 20 \text{ \AA}$  deviate from the straight lines. As is illustrated in the structural characterization, Co layers have hcp phase for  $t_{Co} \geq 25 \text{ \AA}$ , but fcc phase when  $t_{Co}$

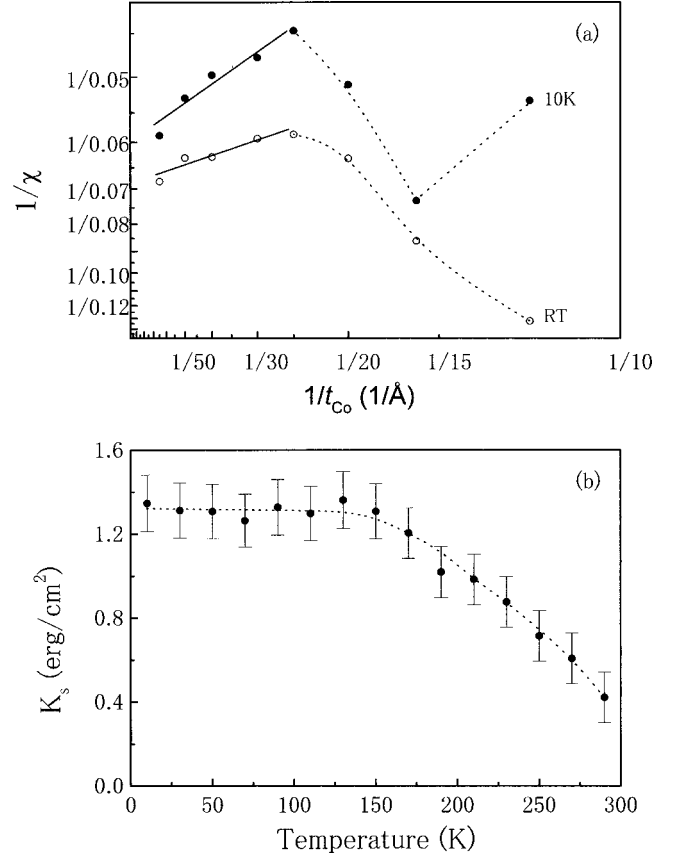


FIG. 6. (a) Plot of the reciprocal  $\chi_0$  as a function of the reciprocal Co thickness at 10 K and room temperature. The solid lines are the fitting results, and the dashed lines are guides to the eye. (b) Temperature dependence of surface anisotropy.

$< 20 \text{ \AA}$ . The magnetic anisotropy for hcp and fcc phase Co is quite different; a varying  $k_v$  is expected for different Co thickness regions with different phases. This is the case of 10 K. On the other hand, thermal agitation destabilizes the direction of magnetization for relatively thin Co layers at elevated temperature, so the susceptibility is not solely determined by the magnetic anisotropy and external field. In Fig. 6(a), the solid lines are the fitting results for the data points of  $t_{Co} \geq 25 \text{ \AA}$ , whereas the dashed lines are guides for the eye. Interesting enough, the line connecting points of  $t_{Co} = 12$  and  $16 \text{ \AA}$  is almost parallel to the fitting line for  $t_{Co} \geq 25 \text{ \AA}$  at 10 K, which suggests that the surface anisotropy does not vary much while Co layers change from fcc to hcp phase. The surface anisotropy was deduced by fitting the data points of  $t_{Co} \geq 25 \text{ \AA}$ . Figure 6(b) shows the temperature dependence of the surface anisotropy in MgO/Co multilayers. The surface anisotropy was found to be as high as  $1.3 \pm 0.2 \text{ erg/cm}^2$  with the film normal as the hard axis at 10 K, which monotonically decreases to  $0.4 \pm 0.2 \text{ erg/cm}^2$  when the samples are warmed up to room temperature. We would like to point out that the *perpendicular susceptibility* method is a very simple way to determine the surface anisotropy with no need of a high field. In order to verify its validity, the surface anisotropy is derived from the  $M$ - $H$  curves along the per-

pendicular direction, which leads to the same result as the *perpendicular susceptibility* method.

Large surface anisotropy in MgO/Co multilayers is thus well defined. One may question how the surface anisotropy, which should be isotropic in the film plane, can affect the in-plane hysteresis behavior. Interface roughness and defects seem to play a crucial role, which inevitably create random inhomogeneities to induce local anisotropy. Bruno *et al.*<sup>19</sup> has ever stressed the importance of the roughness while dealing with the hysteresis properties of the ultrathin films with perpendicular magnetization. Making simple assumptions regarding thickness fluctuations as the nature of domain wall pinning, he derived a coercivity  $H_C \propto 1/t^{5/2}$  where  $t$  is the thickness of the magnetic layer. The epitaxial Pd(111)/Co/Pd (Ref. 20) and Au/Co/Au (Ref. 19) were found to follow the theoretical prediction fairly good. However, neither epitaxial Pt(111)/Co/Pt (Ref. 21) nor Co/Pd superlattices<sup>22</sup> were consistent with Bruno's theory, and the latter, in fact, exhibit a linear dependence of  $H_C$  on  $1/t_{Co}$ . The coercivity is mostly determined by the microstructures at the interface for the multilayers with either perpendicular or planar magnetization. A further quantitative interpretation of the correlation of coercivity and surface anisotropy in MgO/Co multilayers is beyond the scope of this article.

## V. SUMMARY

MgO/Co multilayer films with fairly good layer structure have been fabricated by sputtering. These films show planar magnetization. Coercivity of higher than 12 kOe was found at 10 K for the film with Co thickness of 12 Å. The thickness dependence of coercivity at 10 K follows a linear scale as  $1/t_{Co}$ . The coercivity decreases as temperature rises. Based upon initial susceptibility measurements, a very simple way to determine the surface anisotropy was proposed. A large surface anisotropy was found to account for the hysteresis behavior of MgO/Co multilayer films, especially at low temperature.

## ACKNOWLEDGMENTS

J.W.C. wishes to thank Dr. Endo, Mr. Sakurai, and Mr. Kikuchi at RISM of Tohoku University for their kind help during the sample preparation and magnetic measurements. We are very grateful to Dr. Tsutomu Nojima at Center for Low Temperature Science, Tohoku University for performing high field measurements. This work was supported by the Research for the Future Program of Japan Society for the Promotion of Science under Grant No. 97R14701.

<sup>1</sup>D. N. Lambeth, E. M. T. Velu, G. H. Bellesis, L. L. Lee, and D. E. Laughlin, *J. Appl. Phys.* **79**, 4496 (1996).

<sup>2</sup>M. Yu, M. F. Doerner, and D. J. Sellmyer, *IEEE Trans. Magn. MAG-34*, 1534 (1998).

<sup>3</sup>R. A. McCurrie and P. Gaunt, *Philos. Mag.* **13**, 567 (1966); **19**, 339 (1969).

<sup>4</sup>O. A. Ivanov, L. V. Solina, V. A. Demshina, and L. M. Magat, *Phys. Met. Metallogr.* **35**, 81 (1973).

<sup>5</sup>S. Stavroyiannis, I. Panagiotopoulos, D. Niarchos, J. A. Christodoulides, Y. Zhang, and G. C. Hadjipanayis, *Appl. Phys. Lett.* **73**, 3453 (1998).

<sup>6</sup>M. Yu, Y. Liu, A. Moser, D. Weller, and D. J. Sellmyer, *Appl. Phys. Lett.* **75**, 3992 (1999).

<sup>7</sup>C. P. Luo and D. J. Sellmyer, *Appl. Phys. Lett.* **75**, 3162 (1999).

<sup>8</sup>C. M. Kuo and P. C. Kuo, *J. Appl. Phys.* **87**, 419 (2000).

<sup>9</sup>See the various contributions to *Ultrathin Magnetic Structures*, edited by J. A. C. Bland and B. Heinrich (Springer-Verlag, Berlin, 1994).

<sup>10</sup>M. H. Wiedmann, B. N. Engel, and C. M. Falco, *J. Appl. Phys.* **76**, 6075 (1994).

<sup>11</sup>C. Chen, O. Kitakami, and Y. Shimada, *J. Appl. Phys.* **84**, 2184 (1998).

<sup>12</sup>M. Sharma, S. X. Wang, and J. H. Nickel, *Phys. Rev. Lett.* **82**,

616 (1999).

<sup>13</sup>J. M. De Teresa, A. Barthélémy, A. Fert, J. P. Contour, F. Montaigne, and P. Seneor, *Science* **286**, 507 (1999); J. M. De Teresa, A. Barthélémy, A. Fert, J. P. Contour, R. Lyonnnet, F. Montaigne, P. Seneor, and A. Vaures, *Phys. Rev. Lett.* **82**, 4288 (1999).

<sup>14</sup>H. Lüth, *Surface and Interfaces of Solid Materials*, 3rd ed. (Springer, Berlin, 1995), p. 119.

<sup>15</sup>S. Craig and G. L. Harding, *J. Vac. Sci. Technol.* **19**, 205 (1981).

<sup>16</sup>K. L. Chopra, *Thin Film Phenomena* (McGraw-Hill, New York, 1969), p. 138.

<sup>17</sup>P. Gaunt, *Philos. Mag. B* **48**, 261 (1983).

<sup>18</sup>P. M. L. Néel, *J. Phys. Radium* **15**, 225 (1954).

<sup>19</sup>P. Bruno, G. Bayreuther, P. Beauvillain, C. Chappert, G. Lugert, D. Renard, J. P. Renard, and J. Seiden, *J. Appl. Phys.* **68**, 5759 (1990).

<sup>20</sup>S. T. Purcell, M. T. Johnson, N. W. E. McGee, J. J. de Vries, W. B. Zeper, and W. Hoving, *J. Appl. Phys.* **73**, 1360 (1993).

<sup>21</sup>N. W. E. McGee, M. T. Johnson, J. J. de Vries, and J. aan de Stegge, *J. Appl. Phys.* **73**, 3418 (1993).

<sup>22</sup>B. N. Engel, C. D. England, R. V. Leeuwen, M. Nakada, and C. M. Falco, *J. Appl. Phys.* **69**, 5643 (1991).